Defect studies in annealed ZnO by positron annihilation spectroscopy

2008 J. Phys.: Condens. Matter 20 045217

(http://iopscience.iop.org/0953-8984/20/4/045217)

J. Phys.: Condens. Matter **20** (2008) 045217 (4pp) doi:10.1088/0953-8984/20/04/045217

Defect studies in annealed ZnO by positron annihilation spectroscopy

D Sanyal, Tapatee Kundu Roy, Mahuya Chakrabarti, Siddhartha Dechoudhury, Debasis Bhowmick and Alok Chakrabarti

Variable Energy Cyclotron Centre, 1/AF, Bidhannagar, Kolkata 700064, India

E-mail: dirtha@veccal.ernet.in (D Sanyal)

Received 9 November 2007, in final form 4 December 2007
Published 8 January 2008
Online at stacks.iop.org/JPhysCM/20/045217

Abstract

Coincidence Doppler broadening of the positron annihilation technique has been employed to identify the defects in thermally annealed 'as-received' ZnO and thermally annealed ball-milled nanocrystalline ZnO. Results indicate that a significant amount of oxygen vacancy has been created in ZnO due to annealing at about 500 °C and above. The results also indicate that the Zn vacancy created during the ball milling process can be easily removed by annealing the sample at about 500 °C and above. The defect characterization has also been correlated with the magnetic properties of ZnO.

(Some figures in this article are in colour only in the electronic version)

1. Introduction

Recently, ZnO and a few other oxides have received a lot of attention following the prediction [1] that ferromagnetic ordering above room temperature could be possible by doping a very low amount ($\leqslant$4 at.%) of transition metal ion (Mn, Co, Fe, etc) into these oxides. These materials offer the advantages of semiconductors combined with the non-volatile properties of magnetic materials and thus they have a number of potentially interesting device applications [2]. Since then, an enormous amount of experimental effort [3–8] has been put forward to make diluted magnetic semiconductor (DMS) by doping different 3d transition metal ion e.g. Mn, Fe, Co, etc, into ZnO. Interestingly, room-temperature ferromagnetic ordering in the Mn-doped ZnO system has been observed for those samples that are sintered in between temperatures of 400 and 550 °C [3, 4]. Recently, room-temperature ferromagnetism has been observed in undoped nanocrystalline ZnO [9, 10]. It is clearly indicated [10] that the oxygen vacancies present at the surface of this nanocrystalline ZnO are mainly responsible for the room-temperature ferromagnetism in nanocrystalline ZnO. Oxygen vacancies also enhance the room-temperature ferromagnetism in ZnO-based DMS system [11]. Thus it is very important to characterize both Zn as well as oxygen vacancy-type defects in ZnO. The main motivation of the present work is the systematic study of defects introduced in ZnO as a function of annealing temperature and to correlate the magnetic properties of ZnO with the defects.

Defects can be introduced into a material by various methods. The most common method is by doping with impurity atoms. One can introduce controlled defects in a system by thermal treatment [10, 12, 13] or by using an energetic ion beam [14, 15]. In the present study, 'as-received' ZnO powder has been ball-milled to achieve an average particle size of ∼15 nm. During the preparation of nanocrystalline oxides by the ball milling process, a large number of defects are introduced inside the material [16, 17]. In the nanocrystalline phase, since the surface-to-volume ratio is very high, the surface defects play an important role. The ball-milled ZnO (nano-ZnO powder) and the 'as-received' ZnO (submicron ZnO powder) have subsequently been annealed at different temperatures (150–600 °C) in air.

The positron annihilation technique [18, 19] has been used widely to characterize defects in samples like ZnO [20–24]. For the characterization of defects in the different ZnO samples, coincidence Doppler broadening of the annihilation radiation (CDBAR) measurement technique has been employed. In the CDBAR spectroscopic technique, a positron from the radioactive (^{22}Na) source is thermalized inside the material under study and it annihilates with an electron, emitting two oppositely directed 511 keV γ-rays [18, 19]. Depending upon the momentum of the electron (p), these 511 keV γ-rays are

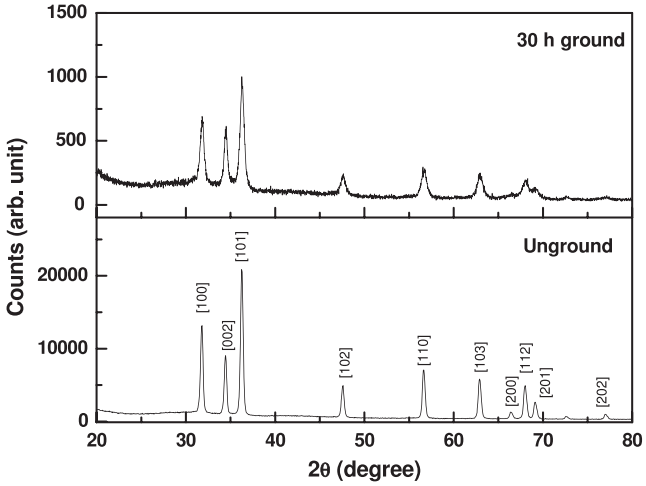

Figure 1. X-ray diffraction pattern for the unground (as-received) and 30 h ball-milled ZnO samples.

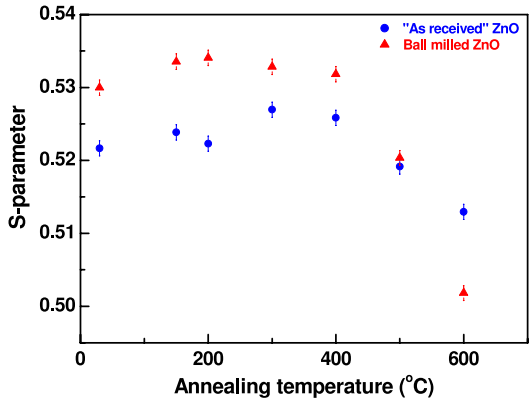

Figure 2. Variation in the *S*-parameter with annealing temperature for both the 'as-received' and 30 h ball-milled ZnO samples.

Doppler shifted by an amount $\pm\Delta E$ in the laboratory frame, where $\Delta E = p_L c/2$, with p_L being the component of the electron momentum, p, towards the detector direction. By using two identical high-resolution HPGe detectors, one can measure the lineshape of these 511 keV γ-rays. The wing part of the 511 keV photo peak carries information about the annihilation of positrons with higher-momentum electrons, e.g. core electrons of different atoms. Thus, by measuring the Doppler broadening of the 511 keV γ-ray and appropriate analysis of the CDBAR spectrum [21, 25–27], one can identify the electrons with which positrons are annihilating and hence the atoms surrounding a defect.

2. Experimental outline

ZnO powder of purity 99.998% from Alfa Aesar, Johnson Matthey, Germany have been ball-milled in a Fritsch Pulverisette 5 planetary ball mill grinder with agate balls for 30 h to achieve an average particle size of ∼15 nm. The as-received ZnO powder and the 30 h ball-milled ZnO powder were then annealed at different temperature of 150, 200, 300, 400, 500 and 600 °C in air for a constant duration (5 h). To avoid any type of stress and strain, slow heating and cooling (at the rate of 3 °C min^{-1}) was always maintained.

The x-ray diffraction (XRD) data are collected on a Philips PW 1710 automatic diffractometer with Cu Kα radiation. For each sample, a scan has been performed from 4° to 90° with a step size of 0.02°. The particle size of the sample has been calculated from the Scherrer formula [28], i.e.

$$D = K\lambda/\beta\cos\theta$$

where D is the particle size, β is the width, K is a constant (= 0.89), λ is the wavelength and θ is the Bragg angle.

For the CDBAR measurement, two identical HPGe detectors (efficiency, 12%; type, PGC 1216sp from DSG, Germany) with an energy resolution of 1.1 at 514 keV of ^{85}Sr, have been used as two 511 keV γ-ray detectors. The CDBAR spectrum have been recorded in a dual ADC-based multiparameter data acquisition system (MPA-3 from FAST ComTec, Germany). A 10 μCi ^{22}Na positron source (enclosed in thin Mylar foil) has been sandwiched between two identical and plane-faced pellets [10, 29]. The peak-to-background ratio of this CDBAR measurement system, with $\pm\Delta E$ selection, is $\sim 10^5$:1.

The coincidence Doppler broadening of the annihilation 511 keV γ-ray spectrum has been analyzed by evaluating the conventional lineshape parameters (*S*-parameter) [18, 19]. The *S*-parameter is calculated as the ratio of the counts in the central area of the 511 keV photo peak ($|511\text{ keV} - E_\gamma| \leqslant 0.85$ keV) and the total area of the photo peak ($|511\text{ keV} - E_\gamma| \leqslant 4.25$ keV). The *S*-parameter represents the fraction of positrons annihilating with the lower momentum electrons with respect to the total electrons annihilated. CDBAR spectra have also been analyzed by constructing the ratio curve [21, 25–27] with respect to the CDBAR spectrum of Al (defect-free 99.9999%-purity) single crystal.

The magnetization measurements were performed in a MPMS-XL superconducting quantum interference device (SQUID) Quantum Design magnetometer.

3. Results and discussion

Figure 1 shows the XRD patterns for the unground (as-received) and the 30 h ball-milled samples. The average particle sizes, as calculated from the Scherrer formula, are 107 and 15 nm for unground and 30 h ball-milled samples, respectively.

Figure 2 represents the *S*-parameter for the 'as-received' ZnO and nanocrystalline ZnO (30 h ball-milled) versus annealing temperature. It is clear from figure 2 that the *S*-parameter has a higher value for 30 h ball-milled ZnO (nanocrystalline ZnO) than the 'as-received' ZnO. The *S*-parameter for both the samples ('as-received' ZnO and ball-milled ZnO) increases slowly up to an annealing temperature of 300 °C, and after that it decreases. The amount of decrease in the *S*-parameter is more in the case of 30 h ball-milled ZnO than the unground ZnO. The *S*-parameter represents the fraction of positrons annihilating with the lower-momentum

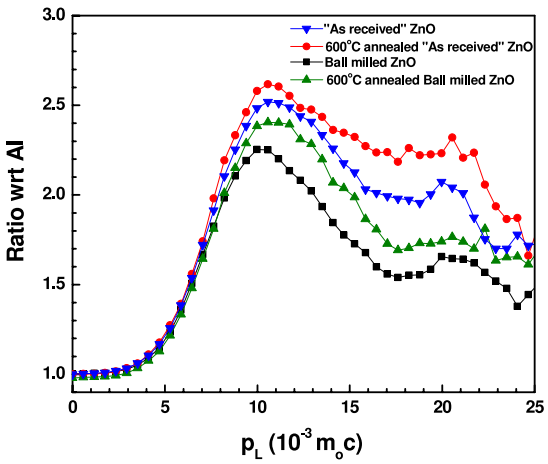

Figure 3. Ratio of the experimental electron–positron momentum distributions for different ZnO samples to the electron–positron momentum distributions for the defect-free Al (99.9999%-purity) single crystal.

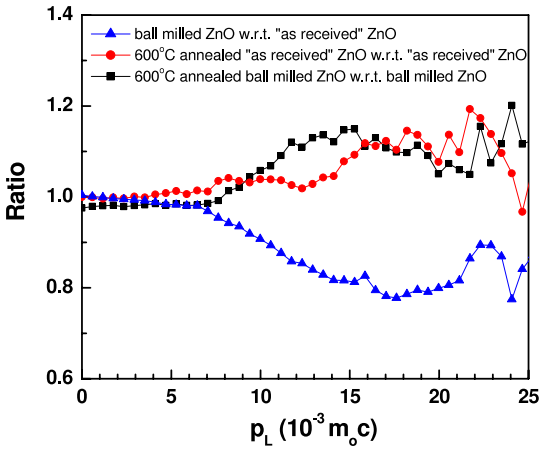

Figure 4. Ratio of the experimental electron–positron momentum distributions for different ZnO samples.

electrons with respect to the total electrons annihilated. The higher value of the *S*-parameter for the 30 h ball-milled ZnO indicates more annihilation of positrons in the defect sites, e.g. Zn vacancies. The slow increase in the *S*-parameter with annealing temperature indicates the enhancement of the open volume defects in ZnO. The decrease in the *S*-parameter after 400 °C suggests that positrons are annihilating more with the higher-momentum electrons, e.g. core electrons. For a better understanding, CDBAR spectra have been analyzed by constructing the ratio curve [21, 25–27] with respect to the CDBAR spectrum of Al (defect-free 99.9999%-purity) single crystal. Figure 3 represents the ratio curves for the 'as-received' ZnO, 600 °C annealed 'as-received' ZnO, ball-milled ZnO and 600 °C annealed ball-milled ZnO with respect to Al single crystal. Also, ratio curves have been plotted (figure 4) for the CDBAR spectrum of the ball-milled ZnO with respect to the CDBAR spectrum of 'as-received' ZnO and CDBAR spectra of annealed ZnO with the corresponding un-annealed ZnO. All the ratio curves (figure 3) show a peak at $\sim 10 \times 10^{-3}\ m_0c$, and a shoulder-type peak at $\sim 21 \times 10^{-3}\ m_0c$. It is clear from figure 3 that, due to ball milling, both the peaks at $\sim 10 \times 10^{-3}\ m_0c$ and at $\sim 21 \times 10^{-3}\ m_0c$ reduce, but for both ball-milled and 'as-received' ZnO, due to annealing at 600 °C, the ratio peaks at $10 \times 10^{-3}\ m_0c$ and at $\sim 21 \times 10^{-3}\ m_0c$ increases. Using the relation $E = p^2/4m_o$, the kinetic energies of electrons corresponding to momentum $p_L \sim 10 \times 10^{-3}\ m_0c$ and $21 \times 10^{-3}\ m_0c$ comes out to be ∼13 and 56 eV, respectively. Thus the annihilation of positrons with oxygen 2p and Zn 3d core electrons contributes to the peak at $10 \times 10^{-3}\ m_0c$, and the peak at $\sim 21 \times 10^{-3}\ m_0c$ comes solely from the annihilation of positrons with 3p core electrons of Zn. In figure 4, the ratio curve for the ball-milled ZnO with respect to unmilled ZnO shows a broad dip from the momentum range $\sim 7 \times 10^{-3}$ to $\sim 23 \times 10^{-3}\ m_0c$. In the same momentum range ($\sim 7 \times 10^{-3}$ to $\sim 23 \times 10^{-3}\ m_0c$), for the annealed ZnO a broad peak has been observed. Thus from figures 3 and 4 it is seen that for the ball-milled ZnO, positrons annihilate less with the core electrons (both 3d and 3p) of Zn. This indicates the formation of cation-type defects (Zn vacancy) in the ZnO system due to ball milling. This observation is in agreement with our previous observations of the formation of cation-type defects in other oxides due to the reduction of the particle size by the ball milling process [16, 17].

The most important feature of figure 2 is that, in both cases ('as-received' or unground and 30 h ball-milled), the *S*-parameter decreases largely due to annealing above 500 °C. This feature is also prominent in the ratio curves (figures 3 and 4). Figures 3 and 4 clearly indicate that, due to annealing at 600 °C, positrons annihilate more with the core electrons (both 3p and 3d) of the Zn atom. The increase in positron annihilations with the core electrons (both 3d and 3p) of Zn suggests that, due to annealing at 600 °C, the Zn vacancies present in the 30 h ball-milled ZnO sample disappear. Also, a significant amount of oxygen vacancies has been created in both samples ('as-received' ZnO and 30 h ball-milled ZnO) due to annealing at 600 °C. This is in agreement with the earlier work [10, 21, 22]. Dutta *et al*, [21] has observed that in polycrystalline ZnO, the Zn vacancy predominates up to an annealing temperature of 300 °C but, due to further annealing, more and more oxygen vacancies are generated in ZnO. Selim *et al*, [30] has also observed the formation of the oxygen vacancy in ZnO due to annealing.

To understand the room-temperature magnetic properties of the differently prepared ZnO, the SQUID measurement technique has been employed. Figure 5 represents the room-temperature magnetic properties of the 'as-received' ZnO, 30 h ground ZnO and 600 °C annealed 'as-received' ZnO. It is observed from figure 5 that the 30 h ground ZnO is more diamagnetic than the 'as-received' ZnO. Moreover, from the positron annihilation technique, it has been observed that the Zn vacancy is in the 30 h ground ZnO more than the 'as-received' ZnO. This suggests that the Zn vacancy in the undoped ZnO system may enhance its diamagnetic nature. Figure 5 also shows that, due to annealing at 600 °C, the 'as-received' ZnO becomes less diamagnetic (up to an applied magnetic field of 3 kOe). Positron annihilation characterization for these samples indicates that, due to annealing at about

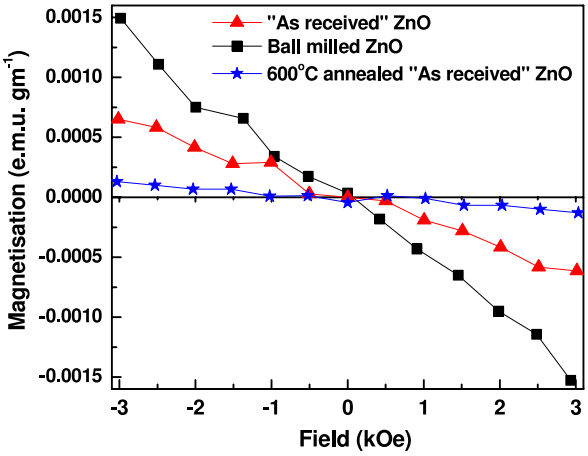

Figure 5. Room-temperature magnetization curves for different ZnO samples.

600 °C, oxygen vacancies have been introduced in the 'as-received' ZnO system. It is interesting to note that the average particle size of the 'as-received' ZnO is ∼107 nm. Previously, it has been observed [10] that the oxygen vacancy in nanocrystalline ZnO makes it ferromagnetic. But, in the present case, it has been observed that the introduction of oxygen vacancies even changes the room-temperature magnetic properties of the 'as-received' ZnO. In a number of papers it has been shown experimentally [9–11] that the magnetic properties of ZnO and transition metal ion doped ZnO significantly changes with oxygen vacancy. Also, there are some experimental and theoretical works [31, 32] where some correlation between different defects with the magnetic properties of transition metal ion doped ZnO has been made but, in the case of undoped ZnO, a theoretical understanding is still not clear.

4. Conclusion

Defects introduced in ZnO due to ball milling and annealing processes have been characterized by employing coincidence Doppler broadening of the annihilation radiation spectroscopic technique. The results indicate that the Zn vacancies, created during the ball milling process, can easily be removed by annealing the sample at about 500 °C and above. The present observation also indicates that the presence of Zn vacancy makes ZnO more diamagnetic and, by annealing at 600 °C, one can introduce oxygen vacancies in ZnO, which makes 'as-received' (submicron) ZnO less diamagnetic.

Acknowledgment

One of the authors, M Chakrabarti, gratefully acknowledges the Council of Scientific and Industrial Research, Government of India, for providing financial assistance.

References

[1] Dietl T, Ohno H, Matsukura F, Gilbert J and Ferrand D 2000 *Science* **287** 1019
[2] Wolf S A, Awschalom D D, Buhrman R A, Daughton J M, Von Molnar S, Roukes M L, Chtchelkanova A Y and Treger D M 2001 *Science* **294** 1488
[3] Sharma P, Gupta A, Rao K V, Owens F J, Sharma R, Ahuja R, Osorio Guillen J M, Johansson B and Gehring G A 2003 *Nat. Mater.* **2** 673
[4] Kundaliya D C, Ogale S B, Loflanf S E, Dhar S, Metting C J, Shinde S R, Ma Z, Varughese B, Ramanujachary K V, Salamanca-Riba L and Venkatesan T 2004 *Nat. Mater.* **3** 709
[5] Zhang J, Skomski R and Sellmyer D J 2005 *J. Appl. Phys.* **97** 10D303
[6] Han S-J, Song J W, Yang C H, Park S H, Park J H, Jeong Y H and Rhie K W 2002 *Appl. Phys. Lett.* **81** 4212
[7] Tanaka K, Fukui K, Murai S and Fujita K 2006 *Appl. Phys. Lett.* **89** 052501
[8] Karmakar D, Mandal S K, Kadam R M, Paulose P L, Rajarajan A K, Nath T K, Das A K, Dasgupta I and Das G P 2007 *Phys. Rev.* B **75** 144404
[9] Sundaresan A, Bhargavi R, Rangarajan N, Siddesh U and Rao C N R 2006 *Phys. Rev.* B **74** 161306(R)
[10] Sanyal D, Chakrabarti M, Roy T K and Chakrabarti A 2007 *Phys. Lett.* A **371** 482
[11] Hsu H S, Huang J C A, Huang Y H, Liao T F, Lin M Z, Lee C H, Lee J F, Chen S F, Lai L Y and Liu C O 2006 *Appl. Phys. Lett.* **88** 242507
[12] Hur T B, Jeen G S, Hwang Y H and Kim H K 2003 *J. Appl. Phys.* **94** 5787
[13] Chen Z Q, Yamamoto S, Maekawa M, Kawasuso A, Yuan X L and Sekiguchi T 2003 *J. Appl. Phys.* **94** 4807
[14] Chen Z Q, Wang S J, Maekawa M, Kawasuso A, Naramoto H, Yuan X L and Sekiguchi T 2007 *Phys. Rev.* B **75** 245206
[15] Brunner S, Puff W, Mascher P and Balogh A G 1999 *Mater. Res. Soc. Symp. Proc.* **540** 207
[16] Chakrabarti M, Dutta S, Chattopadhayay S, Sarkar A, Sanyal D and Chakrabarti A 2004 *Nanotechnology* **15** 1792
[17] Chakrabarti M, Bhowmick D, Sarkar A, Chattopadhyay S, Dechoudhury S, Sanyal D and Chakrabarti A 2005 *J. Mater. Sci.* **40** 5265
[18] Hautojärvi P and Corbel C 1995 *Positron Spectroscopy of Solids* ed A Dupasquier and A P Mills Jr (Amsterdam: IOS Press) p 491
[19] Krause-Rehberg R and Leipner H S 1999 *Positron Annihilation in Semiconductors* (Berlin: Springer) chapter 3, p 61
[20] Tuomisto F, Ranki V, Saarinen K and Look D C 2003 *Phys. Rev. Lett.* **91** 205502
[21] Dutta S, Chakrabarti M, Jana D, Sanyal D and Sarkar A 2005 *J. Appl. Phys.* **98** 053513
[22] Dutta S, Chattopadhyay S, Sutradhar M, Sarkar A, Chakrabarti M, Sanyal D and Jana D 2007 *J. Phys.: Condens. Matter* **19** 236218
[23] Brauer G, Anwand W, Skorupa W, Kuriplach J, Melikhova O and Moisson C 2006 *Phys. Rev.* B **74** 45208
[24] Selim F A, Weber M H, Solodovnikov D and Lynn K G 2007 *Phys. Rev. Lett.* **99** 85502
[25] Asoka-Kumar P, Alatalo M, Ghosh V J, Kruseman A C, Nielsen B and Lynn K G 1996 *Phys. Rev. Lett.* **77** 2097
[26] Myler U and Simpson P J 1997 *Phys. Rev.* B **56** 14303
[27] Brusa R S, Deng W, Karwasz G P and Zecca A 2002 *Nucl. Instrum. Methods* B **194** 519
[28] Waren B E 1969 *X-ray Diffraction* (Reading, MA: Addison-Wesley) p 26419
[29] Chakrabarti M, Sanyal D and Chakrabarti A 2007 *J. Phys.: Condens. Matter* **19** 236210
[30] Selim F A, Weber M H, Solodovnikov D and Lynn K G 2007 *Phys. Rev. Lett.* **99** 85502
[31] Hong N H, Sakai J, Huong N T, Poirot N and Ruyter A 2005 *Phys. Rev.* B **72** 45336
[32] Iusan D, Sanyal B and Eriksson O 2006 *Phys. Rev.* B **74** 235208